# Integrating Companding and Deep Learning on Bandwidth-Limited Image Transmission

Heri Prasetyo[1], Alim Wicaksono Hari Prayuda[2], Chih-Hsien Hsia[3*], Muhammad Alif Wisnu[1]

[1] Department of Informatics, Universitas Sebelas Maret (UNS), Indonesia
[2] Department of Electrical Engineering, National Taiwan University of Science and Technology, Taiwan
[3] Department of Computer Science and Information Engineering, National Ilan University, Taiwan
heri.prasetyo@staff.uns.ac.id, wicayudha.wy@gmail.com, chhsia625@gmail.com, kuro.ishida07@student.uns.ac.id

## Abstract

The image companding is a simple image compression technique which is very easy to be implemented in the bandwidth-limited environment. This paper presents a simple way for improving the quality of decompressed image in the image companding task. The proposed method consists of two networks, namely Sub-band Network (SubNet) and Pixel Network (PixNet), for performing an image reconstruction. The SubNet module exploits the effectiveness of Stationary Wavelet Transform (SWT) and Convolutional Neural Network (CNN) in order to recover the lost information in the wavelet sub-bands basis. Whilst, the PixNet part applies CNN with identity mapping to improve the quality of initial reconstructed image obtained from the SubNet module. As reported in this paper, the proposed method outperforms the former existing schemes in the image companding task. It has also been proven that the proposed method is able to improve the quality of reconstructed image with some simple steps.

**Keywords:** Convolutional neural network, Deep learning, Image companding, Residual networks, Stationary wavelet transform

## 1 Introduction

The image companding stands for Compression and Expanding terminology [1]. The image compression reduces the required bits for representing an image in compact form. Whereas, the image expanding recovers back the image from low bits representation into its original number of bits. The image obtained from the expanding stage is often referred as an expanded image. Several methods have been developed and successfully reported for improving the quality of an expanded image. Most of them are with handcrafted features, i.e. all features are simply designed and engineered using formal mathematical calculation. The former scheme in [2] utilizes T-Law technique in order to increase the quality of expanded image. While the method in [3] simply exploits the convolutional sparse representation. Even though they produce a good result, however, their performances are still inferior compared to the former method in [4]. The method in [4] is developed based on the recent advance of deep learning approach.

The deep learning approaches, especially the CNN frameworks, have been effectively and successfully applied for various applications in the image processing and computer vision tasks [4-17]. The CNN framework has driven some huge developments in image companding [4], inverse halftoning [4, 9], image compression [5], super resolution [6], image denoising [7], image enhancement [8], color recovery [10], target detection [11-13], and the other applications. The proposed method presented in this paper is inspired from the successfulness of CNN architecture to increase the quality of expanded image. It is built by integrating the CNN and SWT. The proposed method is suitable to be adopted for bandwidth-limited image transmission as well as in the network requiring the privacy preservation [18], and packet filtering network [19]. The proposed method can also be extended into another applications such as in the image steganography [20], image watermarking [21], etc. Herein, the proposed method can be utilized to reconstruct or estimate the original image from the stego-image or watermarked image. The proposed method performs an end-to-end mapping from stego-image and watermarked image under the SWT and CNN frameworks.

The rest of this paper is then organized as follow: Section II gives introduction about the image companding technique in the bandwidth-limited image transmission. Section III presents the proposed deep learning architecture for improving the quality of expanded image. Section IV reports and discusses the experimental findings obtained from our proposed method. The end of this paper marks the conclusions for the proposed method.

## 2 Image Companding

A brief introduction of image companding is presented in this section along with its application in the bandwidth-limited image transmission. The image companding terminology refers to the usage of image compression and expanding for storage and transmission. The image compression aims to reduce the number of bits for representing each pixel over an image. Whereas, the image expanding forces back the lower bits for each pixel into its original number of bits. For example, suppose that we have an image with 8 bits representation of each pixel. The image compression may decrease this required bits into only 2 bits representation. While, the image expanding performs the hard inverse problem by converting 2

*Corresponding Author: Chih-Hsien Hsia; E-mail: chhsia625@gmail.com
DOI: 10.53106/160792642022052303005

bits representation into 8 bits. Thus, the quality of decoded image is reduced compared to that of the original version.

Let $I$ be an original image of size $M \times N \times C$, where $M$ and $N$ denote an image height and width, respectively. The symbol $C$ presents the number of color channels used to represent the image $I$, i.e. $C = 1$ and $C = 3$ are for grayscale and color space, respectively. Suppose that each pixel over each color channel is represented with $h$ bits. The image compression reduces this required bits into lower bits using the following hard thresholding computation:

$$\hat{I} = \lfloor I/Q \rfloor, \quad \textbf{(1)}$$

where $\hat{I}$ and $\lfloor \cdot \rfloor$ denote the compressed image and mathematical floor operator, respectively. This resulted image is still with the original size, i.e. $M \times N \times C$. The symbol $Q$ indicates a specific quantizer, which is defined as $Q = 2^{h-l}$, where $l$ is the number of bits in lower bit representation. From this computation, the quality of $\hat{I}$ is reduced compared to $I$.

The inverse computation can be performed in order to recover back or estimate the original image from its compressed version $\hat{I}$. This process is formally defined as follow:

$$\tilde{I} = \hat{I}.Q, \quad \textbf{(2)}$$

where $\tilde{I}$ is an expanded image. The size of this image is still identical to that of the original image, i.e. $M \times N \times C$. A simple computation in (2) effectively recovers back an image from lower bits representation $l$ into $h$ high lower bits representation. However, the quality of $\tilde{I}$ is inferior compared to $I$ since of the floor operation in (1). In the subsequent discussions, we refer $\hat{I}$ and $\tilde{I}$ as the Low Definition Range (LDR) image and High Definition Range (HDR) image, respectively.

The image companding technique is very useful in the bandwidth-limited image transmission. Figure 1 illustrates the usage of image companding in bandwidth-limited networks. An original image may not be able to be transmitted in the communication environment with very low or limited bandwidth available. Thus, it is required to reduce the number of bits before transmitting this image. The image compression along with entropy coding can be applied to reduce the required bits of an image. The compressed data-streams with lower bits representation is further transmitted from sender to receiver over the internet network or cloud services. The receiver party simply accepts the compressed data stream. By applying an inverse entropy coding and image expanding techniques, the receiver is able to obtain an expanded image. Thus, the image companding helps two parties for communication over bandwidth-limited network. Figure 2 depicts examples of image companding over various bits. As shown in this figure, the quality of expanded image is degraded compared to that of the original version.

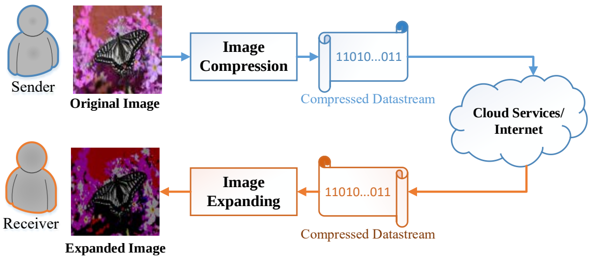


**Figure 1.** Illustration of bandwidth-limited image transmission


**Figure 2.** The original image in 8 bits (a), along with its compression versions over various bits: (b) 2 bits, (c) 3 bits, (d) 4 bits

# 3 Proposed Method

This section presents the proposed method for improving the quality of expanded image. As we know, an expanded image $\tilde{I}$ is with lower quality compared to the original version $I$. The proposed method exploits the deep learning superiority to improve the quality of expanded image. Our goal is to obtain an improved image as similar as possible to the original image. The proposed method consists of Sub-band Networks (SubNet) with DSWT and Pixel Correction Network (PixNet) modules. The full explanation of proposed architecture is given as follow.

## 3.1 Stationary Wavelet Transform

The Stationary Wavelet Transform (SWT) performs image decomposition with un-decimated wavelet basis. It transforms an image into a set of redundant wavelet sub-bands. These redundant sub-bands are the results of avoiding the downsampling and upsampling operations as usually applied in ordinary wavelet transforms. Thus, the resulted image sub-bands are of identical size to the original image. However, the SWT has shortcoming in the translation invariances. Let $A$ be a two dimensional image of size $M \times N$. The SWT decomposes this image as follow:

$$\Im^k\{A_{LL}^{k-1}\} \Rightarrow S = \{A_\theta^k | \theta = LL, LH, HL, HH\}, \quad \textbf{(3)}$$

for $k = 1,2, \ldots, L$, where $A_\theta^k$ and $\Im^k\{\cdot\}$ denote the $k$-level of SWT transformed image sub-band and SWT operator, respectively. We use an initial condition as $A_{LL}^0 = A$ . After applying the SWT over $L$, the set $S$ is now with the size $M \times N \times (3L + 1)$. An example of SWT sub-band is given in Figure 3. It is clear that the SWT sub-band of the original image with 8 bits representation is totally different from SWT sub-band of the expanded image with 2 bits representation. In our proposed method, the information contained in $S$ is very important in the image companding reconstruction.

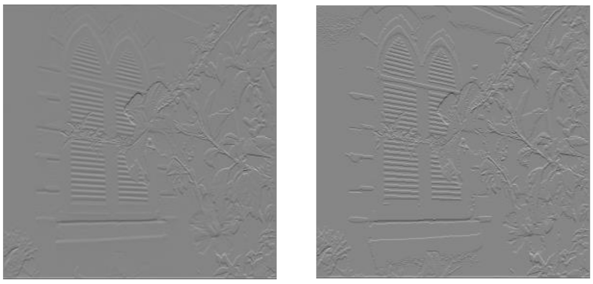

(a) Original image in 8 bits (b) Compressed image in 2 bits

**Figure 3.** The SWT results

The Inverse Stationary Wavelet Transform (ISWT) recovers an image into its original signal with the inverse decomposition technique. The ISWT is formally defined as follow:

$$\mathcal{F}^k \left\{S = \{A_\theta^k | \theta = LL, LH, HL, HH\}\right\} \Rightarrow A^{k-1}, \quad \textbf{(4)}$$

for $k = L, L-1, \ldots, 1$ , where $\mathcal{F}^k\{\cdot\}$ denotes the ISWT operator. The ISWT result is identical or with a slight deteriorate under some extends compared to the original image. In addition, the SWT operation can be directly applied to the color image by processing each color component individually.

## 3.2 Sub-bands Network (SubNet)

The first block in our proposed method is called Sub-bands Network (SubNet) as depicted in the upper part of Figure 4. The SubNet consists of convolution+ReLU [14] layer, a set of residual networks, convolution+ReLU after element-wise addition, and a single convolution layer. It aims to recover the SWT sub-bands from an expanded image or HDR image. The SubNet receives the SWT decomposed sub-bands from an expanded image $\tilde{I}$ as the network input. Let $S$ be a set of SWT sub-bands of expanded image. The $S$ is of size $M \times N \times 3(3L + 1)$, since the expanded image is in three dimensional color space. The SubNet firstly processes the input $S$ individually using convolution+ReLU as follow:

$$x_{in} = \eta(w_{in} * S + b_{in}), \quad \textbf{(5)}$$

where $w_{in}$ and $b_{in}$ are the weights and biases in the input (first) layer. The symbols $*$ and $\eta(\cdot)$ denote the convolution and ReLU operators, respectively. While $x_{in}$ is the feature maps produced from this layer.

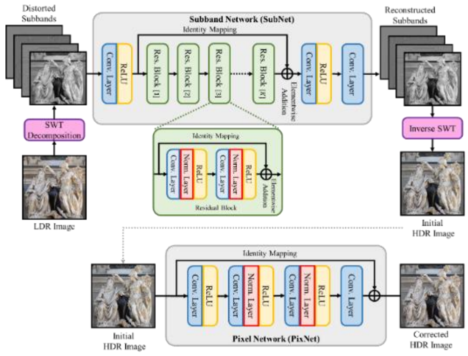


**Figure 4.** Schematic diagram of the proposed method

The SubNet subsequently performs a feature mapping using a set of residual networks, denoted as:

$$x_{D+1} = x_1 + \textstyle\sum_{d=1}^{D} \mathcal{R}(x_d, \theta_d), \quad \textbf{(6)}$$

for $i = 1,2, \ldots, D$ . Where $\mathcal{R}(\cdot)$ is the residual network operator, $x_d$ and $\theta_d$ are the feature maps and network parameters, respectively, at $d$-th layer. Herein, we simply set $x_1 = x_{in}$. A skip connection approach [15] is applied at the end of residual blocks. The element-wise addition between the residual information is performed as follow:

$$x_m = \eta(w_m * [x_{D+1} + x_{in}] + b_m), \quad \textbf{(7)}$$

where $x_m$, $w_m$, and $b_m$ are obtained feature maps, weights, and biases after element wise addition, respectively.

The SubNet finally performs a single convolution layer as follow:

$$S_r = w_o * x_m + b_o, \quad \textbf{(8)}$$

where $w_o$ and $b_o$ are the weights and biases from last (output) layer, respectively. The symbol $S_r$ denotes the reconstructed SWT sub-bands. After applying the ISWT, we obtain an initial reconstructed image $I_r$.

## 3.3 Pixel Correction Network (PixNet)

The PixNet accepts the initial reconstructed image $I_r$ as its input. The PixNet consists of convolution+ReLU, two elements of convolution+normalization layer+ReLU, and a single convolutional layer. These convolutional layers yield a residual information about an enhanced image. An enhanced image can be simply computed by performing element-wise addition by applying an identity mapping [15], as follow:

$$I_e = I_r + I_c, \quad \textbf{(9)}$$

where $I_c$ is the residual information or corrected image after a series of convolutional layers in PixNet, and $I_e$ is the final enhanced image, i.e. the improved quality of expanded image $\tilde{I}$.

The proposed SubNet and PixNet exploit the Mean Squared Error (MSE) as the loss function. This function is exposed during the training process. It measures the network performance as well as gives guidance for the learning process. The loss function of SubNet is in $l_1$-norm. The PixNet employs the $l_2$ -norm loss function with an additional auxiliary Total Variational (TV) over weight $1 \times 10^{-5}$. It is to further suppress the removed detail of an image produced by SubNet.

## 4 Experimental Results

Some experimental results from the proposed method are reported in this section. It includes the report about the parameters tuning for the proposed architecture, the effect of network parameters, visual investigation, and the performance comparisons between the proposed method and the other schemes. For objective measurement, we simply overlook the Peak-Signal-to-Noise Ratio (PSNR) and Structural Similarity Index (SSIM) to measure the similarity between the enhanced image and original image. The enhanced image is also referred as corrected HDR image produced by the proposed networks. Better quality of enhanced image is indicated with higher score of PSNR and SSIM, respectively.

### 4.1 Parameters Tuning for Network Architecture

We firstly perform the parameters tuning for the proposed network architecture and report it in this subsection. The proposed method requires three different image datasets, namely training, validation, and testing sets. The training and validation sets are for the learning purposes. The training set consists of all images downloaded from DIV2K train $\times 3$ and $\times 4$ [16]. While, the validation set is composed from 20 images randomly picked from DIV2K valid $\times 4$ [16]. Figure 5 and Figure 6 show image samples used as training and validation sets, respectively. These two image sets contain a set of images with various underlying information, such as rich image details, colorfull appearances, various image activities, different artistics sides, etc. The prospective readers are suggested to refer the online version of this paper for better visual inspection of all images and experimental results.

**Figure 5.** Some image samples in the training dataset

**Figure 6.** A set of images as validation set

We utilize the Adam optimizer [17] with initial values of $\beta_1$ and $\beta_2$ as 0.9 and 0.999, respectively, to perform the back-propagation of our proposed network. Herein, the proposed SubNet and PixNet architectures use identical learning rate, i.e. $1 \times 10^{-4}$, in which this value is divided by factor 1.5 on every five epochs. The learning process takes the $l_1$ and $l_2$-norm for SubNet and PixNet, respectively, as the loss functions. An instance batch normalization is chosen during the training process, with the batch size 16. We set the number of epochs is 30 indicating that there are about 67K updates performed on the network architectures. In the network parameters tuning, we set the lower bit representation as $l = 4$.

In the first experiment, we investigate the effect of different number of features. Herein, we consider the effect of number of features $N = \{16,32,64\}$, by fixing the number of residual blocks in SubNet as 4. The convolution layers for PixNet are the same as used in Figure 4. Figure 7 displays the loss function in terms of average PSNR values measured from the validation set. As it can be seen from this figure, the number of features $N = 64$ gives the best performance.

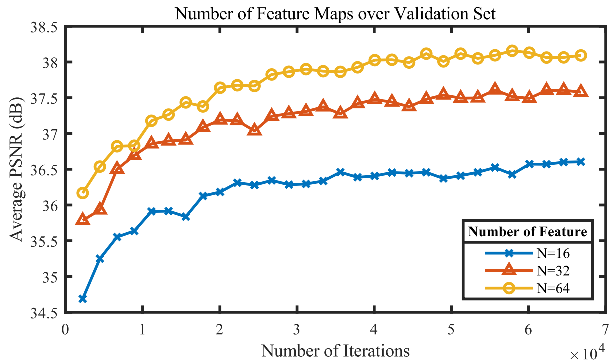


**Figure 7.** Effects of different number of feature maps

Subsequently, we observe the effect of residual blocks on the SubNet. In this experiment, the number of features is set as $N = 64$. The proposed method performance is later examined under various number of residual blocks, i.e. $K = \{2,4,\ldots,10\}$. The number of convolution layers is identically set as used in Figure 4. Figure 8 depicts the loss function obtained from validation set over various number of residual blocks. This figure points out that $K = 6$ yields the best configuration for the number of residual blocks in SubNet. Yet, the proposed method with $N = 64$ and $K = 6$ will be utilized for the later usage in the testing process.

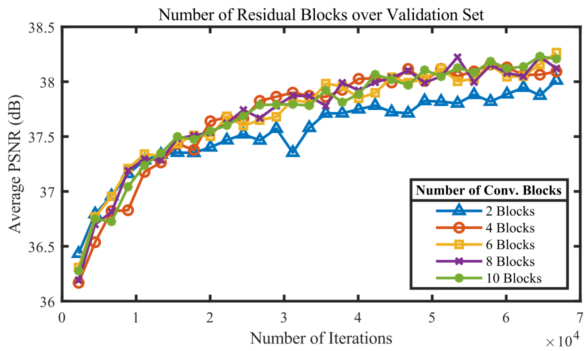


**Figure 8.** Effects of different number of residual blocks

## 4.2 Visual Inspection of Proposed Method

This sub-section reports the proposed method performance visually. All images from the Kodak dataset shown in Figure 9 are turned as testing images. These images are in natural appearance with various color compositions and varieties. The SubNet and PixNet use the optimum parameters setting as obtained in the previous sub-section. In the visual investigation, the quality of enhanced image is simply judged by human vision. Figure 10 and Figure 11 demonstrate the ability of proposed method for enhancing the qualities of Airplane and House images with four bits representation for each pixel, i.e. $l = 4$. Herein, the testing images are with 4 bits representation for LDR image. These two figures show the superiority of the proposed method for enhancing the quality of LDR image in terms of visual inspection. Thus, the proposed method is most preferable in the image companding task compared to the other schemes.

**Figure 9.** A set of testing images from Kodak dataset

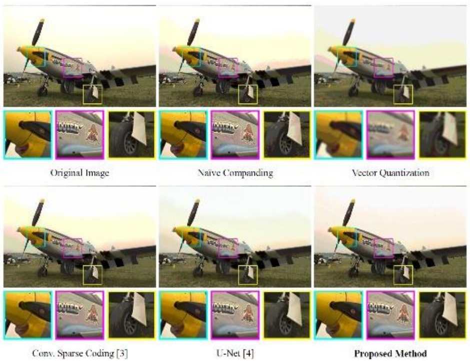


**Figure 10.** Visual comparisons between the proposed method and former schemes on Airplane image


**Figure 11.** Another visual comparisons on House image

## 4.3 Performance Comparisons Against the Former Schemes

An additional experiment is also performed to measure the proposed method performance compared to the former existing schemes. In this experiment, we take all images in the testing set to perform image companding and quality enhancing by executing our proposed network with optimized network parameters. We investigate the proposed method performance by observing various bits representation, i.e. $l = \{2, 3, \ldots, 5\}$. We compute the average PSNR and SSIM scores to further perform comparisons against the former schemes [1, 3-4]. Table 1 and Table 2 tabulate the average PSNR and SSIM scores, respectively, over all testing set. These tables also summarize the comparisons between the proposed method and former schemes [1, 3-4]. In these two tables, the best values are given in the bold face, whereas the second best scores are indicated with the red color. These two tables clearly reveal that the proposed method outperforms the former existing schemes in the image companding scheme as indicated with the highest average PSNR and SSIM values. It can be concluded that the proposed method is the best candidate for image enhancement in the image companding task over bandwidth-limited environment. The proposed method can be simply extended into various applications requiring the reconstruction process such as in the aerospace field, commercial graphics, etc. In the aerospace field, the proposed method can enhance the quality of aerospace objects captured from the sky camera. The proposed method can also improve the quality of degraded image for commercial graphics. Herein, these two problems are similar to the image companding task. They can be regarded as ill-posed inverse imaging problem. Yet, the proposed method is suitable for ill-posed inverse imaging problem.

**Table 1.** Objective performance comparisons in terms of average PSNR

| Methods | 2 bits | 3 bits | 4 bits | 5 bits | Average |
|---|---|---|---|---|---|
| Naïve Companding | 17.49 | 23.48 | 29.75 | 36.17 | 26.72 |
| 2D T-Law [1] | 13.08 | 17.48 | 23.94 | 28.77 | 20.82 |
| Vector Quantization | 22.19 | 24.83 | 25.77 | 27.59 | 25.10 |
| Conv. Sparse Coding [3] | 22.22 | 30.49 | 34.11 | 35.41 | 30.56 |
| U-Net [4] | 22.23 | 30.50 | 36.22 | 41.16 | 32.53 |
| **Proposed Method** | **24.68** | **32.93** | **39.26** | **43.58** | **35.11** |

**Table 2.** Performance comparisons in terms of average SSIM

| Methods | 2 bits | 3 bits | 4 bits | 5 bits | Average |
|---|---|---|---|---|---|
| Naïve Companding | 0.589 | 0.838 | 0.949 | 0.986 | 0.841 |
| 2D T-Law [1] | 0.411 | 0.744 | 0.904 | 0.971 | 0.758 |
| Vector Quantization | 0.637 | 0.775 | 0.831 | 0.876 | 0.780 |
| Conv. Sparse Coding [3] | 0.678 | 0.904 | 0.959 | 0.970 | 0.878 |
| U-Net [4] | 0.670 | 0.905 | 0.964 | 0.989 | 0.882 |
| **Proposed Method** | **0.780** | **0.945** | **0.984** | **0.994** | **0.926** |

# 5 Conclusions

This paper has presented a simple technique for enhancing the quality of expanded image on the bandwidth-limited transmission. The proposed method is developed based on the effectiveness of CNN framework. It consists of two networks, namely SubNet and PixNet. The Experimental Results section validates the superiority of the proposed method in comparisons with the former existing schemes. Thus, the proposed method can be plugged as a post-processing step in the image companding over the bandwidth-limited transmission environment.

For the future works, more recent advances in deep learning technique can be exploited to replace the CNN module. The CNN layer in the proposed method can be substituted with recent generative adversarial networks, transformer networks, deep learning networks with visual attentions, and another techniques. The optimization modules including various lost functions can be further investigated to achieve more optimum reconstruction results. In addition, the SWT can also be exchanged with the decimated wavelet or another type of wavelet transformation to yield a better quality on the reconstructed companded image. Another reversible image transformations should be taken into account as another promising option for replacing the wavelet transform.

## References


[1] S. Bhooshan, V. Kumar, 2D T-law: a novel approach for image companding, *Proc. WSEAS International Conference on Circuits, Systems, Signal and Telecommunications*, Cambridge, USA, 2010, pp. 19-22.

[2] S. Bhooshan, V. Kumar, U. Verma, H. Vatsyayan, K. Rohit, T-law: A new suggestion for signal companding, *IEEE Congress on Image and Signal Processing*, Sanya, China, 2008, pp. 190-194.

[3] B. Wohlberg, Convolutional sparse representation of color images, *2016 IEEE Southwest Symposium on Image Analysis and Interpretation (SSIAI)*, Santa Fe, NM, USA, 2016, pp. 57-60.

[4] X. Hou, G. Qiu, *Image Companding and Inverse Halftoning using Deep Convolutional Neural Networks*, July, 2017, https://arxiv.org/abs/1707.00116.

[5] F. Jiang, W. Tao, S. Liu, J. Ren, X. Guo, D. Zhao, An End-to-End Compression Framework Based on Convolutional Neural Networks, *IEEE Transactions on Circuits and Systems for Video Technology*, Vol. 28, No. 10, pp. 3007-3018, October, 2018.

[6] Y. Zou, L. Zhang, C. Liu, B. Wang, Y. Hu, Q. Chen, Super-resolution reconstruction of infrared images based on a convolutional neural network with skip connections, *Optics and Lasers in Engineering*, Vol. 146, Article No. 106717, November, 2021.

[7] L. Liang, S. Deng, L. Gueguen, M. Wei, X. Wu, J. Qin, Convolutional neural network with median layers for denoising salt-and-pepper contaminations, *Neurocomputing*, Vol. 442, pp. 26-35, June, 2021.

[8] H. Prasetyo, A. W. H. Prayuda, C.-H. Hsia, J.-M. Guo, Deep Concatenated Residual Networks for Improving Quality of Halftoning-Based BTC Decoded Image, *Journal of Imaging*, Vol. 7, No. 2, Article No. 13, February, 2021.

[9] H. P. A. Wicaksono, H. Prasetyo, J.-M. Guo, Deep Learning based Inverse Halftoning via Stationary Wavelet Domain, *2020 27th International Conference on Telecommunications (ICT)*, Bali, Indonesia, 2020, pp. 1-5.

[10] A. R. Bagaskara, H. Prasetyo, H. P. A. Wicaksono, Color-embedded-grayscale quality enhancement using deep convolutional networks, *2020 27th International Conference on Telecommunications (ICT)*, Bali, Indonesia, 2020, pp. 1-5.

[11] Y. Li, K. Liu, W. Zhao, Y. Huang, Target Detection Method for SAR Images Based on Feature Fusion Convolutional Neural Network, *Journal of Internet Technology*, Vol. 21, No. 3, pp. 863-870, May, 2020.

[12] Y. Li, H. Li, X. Li, X. Li, P. Xie, On Deep Learning Models for Detection of Thunderstorm Gale, *Journal of Internet Technology*, Vol. 21, No. 4, pp. 909-917, July, 2020.

[13] S. Vimal, Y. H. Robinson, S. Kadry, H. V. Long, Y. Nam, IoT Based Smart Health Monitoring with CNN Using Edge Computing, *Journal of Internet Technology*, Vol. 22, No. 1, pp. 173-185, January, 2021.

[14] K. He, X. Zhang, S. Ren, J. Sun, *Delving Deep into Rectifiers: Surpassing Human-Level Performance on ImageNet Classification*, February, 2015, https://arxiv.org/abs/1502.01852.

[15] K. He, X. Zhang, S. Ren, J. Sun, Identity Mappings in Deep Residual Networks, arXiv:1603.05027, July, 2016.

[16] E. Agustsson, R. Timofte, NTIRE 2017 Challenge on Single Image Super-Resolution: Dataset and Study, *2017 IEEE Conference on Computer Vision and Pattern Recognition Workshops (CVPRW)*, Honolulu, HI, USA, 2017, pp. 1122-1131.

[17] D. P. Kingma, J. Ba, *Adam: A Method for Stochastic Optimization*, January, 2017, https://arxiv.org/abs/1412.6980.

[18] A. I. Basuki, D. Rosiyadi, I. Setiawan, Preserving Network Privacy on Fine-grain Path-tracking using P4-based SDN, *2020 International Conference on Radar, Antenna, Microwave, Electronics, and Telecommunications (ICRAMET)*, Tangerang, Indonesia, 2020, pp. 129-134.

[19] F. M. Wibowo, M. F. Sidiq, I. A. Akbar, A. I. Basuki, D. Rosiyadi, Collaborative Whitelist Packet Filtering Driven by Smart Contract Forum, *2019 International Seminar on Research of Information Technology and Intelligent Systems (ISRITI)*, Yogyakarta, Indonesia, 2019, pp. 205-210.

[20] A. I. Basuki, D. Rosiyadi, Joint Transaction-Image Steganography for High Capacity Covert Communication, *2019 International Conference on Computer, Control, Informatics and its Applications (IC3INA)*, Tangerang, Indonesia, 2019, pp. 41-46.

[21] D. Rosiyadi, H. Prasetyo, S. J. Horng, A. I. Basuki, Security Attack on Secret Sharing Based Watermarking Using Fractional Fourier Transform and Singular Value Decomposition, *2020 International Conference on Radar, Antenna, Microwave, Electronics, and Telecommunications (ICRAMET)*, Tangerang, Indonesia, 2020, pp. 343-347.


## Biographies

**Heri Prasetyo** received his Bachelor's Degree from the Department of Informatics Engineering, Institut Teknologi Sepuluh Nopember (ITS), Indonesia in 2006. He received his Master's and Doctoral Degrees from the Department of Computer Science and Information Engineering, and Department of Electrical Engineering, respectively, at the National Taiwan University of Science and Technology (NTUST), Taiwan, in 2009 and 2015, respectively. He received the Best Dissertation Award from the Taiwan Association for Consumer Electronics (TACE) in 2015, Best Paper Awards from the International Symposium on Electronics and Smart Devices 2017 (ISESD 2017), ISESD 2019, and International Conference on Science in Information Technology (ICSITech 2019), and the Outstanding Faculty Award 2019 from his current affiliated university. His research interests include multimedia signal processing, computational intelligence, pattern recognition, and machine learning.

**Alim Wicaksono Hari Prayuda** received the bachelor degree from the Universitas Sebelas Maret (UNS), Indonesia, in 2020. He is currently working toward the master degree in Department of Electrical Engineering at National Taiwan University of Science and Technology, Taipei, Taiwan. His research interests include Deep Learning application for Digital Image Processing and Multimedia Engineering.

**Chih-Hsien Hsia** was born in Taipei city, Taiwan, in 1979. He received the Ph.D. degree from Tamkang University, New Taipei, Taiwan, in 2010. In 2007, he was a Visiting Scholar with Iowa State University, Ames, IA, USA. From 2010 to 2013, he was a Postdoctoral Research Fellow with the Department of Electrical Engineering, National Taiwan University of Science and Technology, Taipei, Taiwan. From 2013 to 2015, he was an Assistant Professor with the Department of Electrical Engineering at Chinese Culture University, Taiwan. He was an Associate Professor with the Chinese Culture University and National Ilan University from 2015 to 2017. From 2019 to 2020, he was Director, Research Planning Division, Research & Development, National Ilan University, Taiwan. He currently is a Professor and a Chairman with the Department of Computer Science and Information Engineering, National Ilan University, Taiwan. Director, Multimedia & Intelligent Technical Lab., National Ilan University, Taiwan. Dr. Hsia was received the Outstanding Young Scholar Award of the Taiwan Association of Systems Science and Engineering in 2020, the Outstanding Young Scholar Award of the Computer Society of the Republic of China in 2018. His research interests include DSP IC Design, AI in Computer Vision, and Cognitive Learning.
Dr. Hsia is the Chapter Chair of IEEE Young Professionals Group, Taipei Section, and the Director of the IET Taipei Local Network. He has serves on Associate Editor of the Journal of Imaging Science and Technology, the Journal of Imaging, and the Journal of Computers.

**Muhammad Alif Wisnu** received the bachelor degree from the Universitas Sebelas Maret (UNS), Indonesia, in 2022. His research interests include image processing, computer vision, and deep learning.